



A 3D Monte Carlo semiconductor device simulator for submicron silicon MOS transistors¹

K. Tarnay,^{a,b} F. Masszi,^b A. Poppe,^a P. Verhás,^a T. Kocsis,^a
Zs. Kohári^a

^a *Technical University of Budapest, Department of Electron Devices, H-1521 Budapest, Hungary*

^b *Department of Electronics, Institute of Technology, Uppsala University, Box 534, S-751 21 Uppsala, Sweden*

ABSTRACT

A new 3D Monte Carlo simulator has been developed for analyzing the properties of submicron *Si* MOS transistors using the *molecular dynamics* method. This program, called MiCroMOS uses the possible deepest first principles instead of any abstractions or simplifications. In this way, problems arising from the usage of a continuum view, drift-diffusion equations or effective mobility concept are inherently avoided. One of the most important new features of the program is that instead of solving Poisson's equation, the exact potential and electric field caused by the charged particles inside the simulated structure is analytically calculated, resulting in an exact modelling of all Coulomb scattering mechanisms and in real particle trajectories.

¹This research has been sponsored by the Digital Equipment Co. EERP HG-001 and SW-003 projects, and by the Swedish and Hungarian governments' scientific research funds.



NOTATION

$\Psi(\mathbf{r})$	potential at point \mathbf{r}
$\Psi_{imp}(\mathbf{r})$	potential at point \mathbf{r} arising from charged impurities
$\Psi_n(\mathbf{r})$	potential at point \mathbf{r} arising from electrons
$\Psi_p(\mathbf{r})$	potential at point \mathbf{r} arising from holes
$\Psi_{int}(\mathbf{r})$	potential arising from interface charges
$\Psi_B(\mathbf{r})$	potential at point \mathbf{r} caused by applied biases and boundary conditions
$\mathbf{E}_{imp}(\mathbf{r})$	field at point \mathbf{r} caused by charged impurities
$\mathbf{E}_n(\mathbf{r})$	field at point \mathbf{r} caused by electrons
$\mathbf{E}_p(\mathbf{r})$	field at point \mathbf{r} caused by holes
$\mathbf{E}_{int}(\mathbf{r})$	field at point \mathbf{r} caused by interface charges
\underline{m}_{eff}^{-1}	reciprocal effective mass tensor
m_t	transversal effective mass
m_l	longitudinal effective mass
\mathbf{k}	wave vector

INTRODUCTION

Existing Monte Carlo simulators use abstractions and simulate usually only 2D structures. Assuming a silicon MOS structure having a gate area of $1 \times 1 \mu\text{m}^2$ and a doping density of 10^{23}m^{-3} , the number of ionized impurities under the gate in the depletion layer is about 10^3 . The number of inversion carriers is in the same order of magnitude. The relatively small number of carriers and the increasing CPU power of the up-to-date computers suggest the development of a Monte Carlo simulator, where *the trajectories of each carrier are individually followed* both in real space and in \mathbf{k} -space.

Encouraged by the above facts we developed a 3D Monte Carlo simulation program, called MiCroMOS. This program applies the Monte Carlo method for the *active region* only (see Fig. 1). Outside the active region (deep in the source and drain) classical approximations are used.

More precisely, MiCroMOS is a quasi-3D simulator, because in the y -direction artificial boundary conditions are used. Still, the carrier motion is followed in all (even in the y) directions.

The device structure

The program MiCroMOS is a hybrid Monte Carlo simulation in the sense, that a certain part of the source and drain together with the deeper part of the bulk is treated by classical methods, while in the depleted regions (including the inversion channel) forming most of the active region all carriers are examined individually.

Since we have extended the active region simulated by the Monte Carlo method somewhat into the source and drain regions, the computational need of the program has increased. However, this price in CPU time consumption is acceptable in case of shallow junctions ($0.1 - 0.3 \mu\text{m}$ for typical submicron devices).

The latest test version of our program assumes

- graded source and drain junction profiles,
- arbitrary source and drain doping concentrations,
- homogeneous channel and bulk doping concentrations.

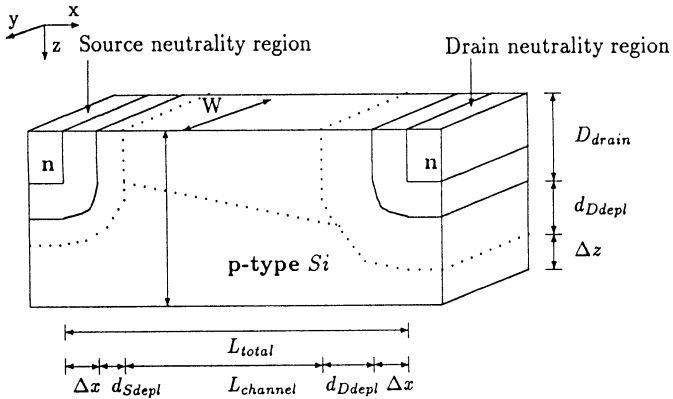


Figure 1: The MOS structure simulated by the MiCroMOS program.

We have to note, that similarly to the way the junction profiles are introduced, inhomogeneous bulk doping may easily be implemented. The dimensions of the examined device (see Fig. 1) are the following:

- On the x-axis: The total length of the calculated structure is the source region plus the channel length (between the source-channel and the channel-drain metallurgical junctions) plus the drain region, where the length of the source region is the sum of a small Δx region and the classically calculated n-side source region. Charge neutrality is forced in that small Δx region.

In a similar way, the length of the drain region is composed of the classically calculated n-side drain depletion region and another small Δx region, in which charge neutrality is forced.

The total length along the x-axis can be expressed as follows:

$$L_{total} = \Delta x + d_{Sdepl} + L_{channel} + d_{Ddepl} + \Delta x$$

- The assumed depth is calculated as follows: The p-side depletion width of the drain-bulk junction is determined by classical approximation. The total depth is given by the sum of the distance of the $Si - SiO_2$ interface to the drain-bulk metallurgical junction, the p-side drain-bulk depletion width and a small Δz region, where charge neutrality is forced.

The total depth considered is the following:

$$D_{total} = D_{drain} + d_{Ddepl} + \Delta z$$

A general assumption is the presence of strong inversion in the channel region. Outside the active region classical approximations are used.

The program has an open structure, thus it is possible to write a more sophisticated control structure (eg. for calculating $I_D - U_{GS}$ characteristics, etc.), to implement new features and/or new physical models, or to replace the present models with new ones.



SIMULATION PRINCIPLES

In addition to the practical considerations already mentioned in the previous section the following considerations have led us to apply the so-called *molecular dynamics* Monte Carlo method for the simulation of submicron semiconductor structures:

- The classical *drift-diffusion* method or the *hydrodynamic method* – both utilizing a continuum view of the transport processes in semiconductor structures (charge transport in the drift-diffusion approach, charge and energy transport in the hydrodynamic approach) – are no more applicable, since in a submicron device structure the number of carriers is in the order of magnitude of a few thousands.
- In the widely used Monte Carlo methods (based on charge clouds, superparticles, etc.) the basic physical phenomena of the simulated system are less pronounced due to the applied sophisticated approximations (eg. distribution functions, scattering rates, Boltzmann transport equation), which can lead to simulated carrier behaviour being incorrect from a physical point of view.

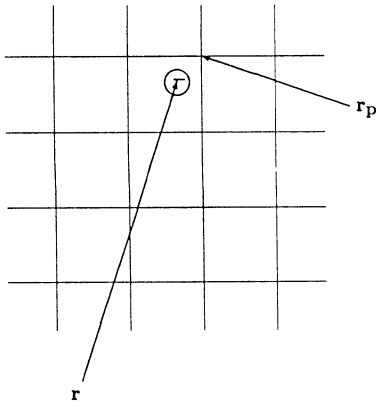
Potential calculation

In our microscopic view, where we consider point charges the "life" of which is followed individually, using Poisson's equation would cause major problems.

Problems with Poisson's equation. Solving Poisson's equation requires that a 2D or 3D grid is generated. An effective charge density is assigned to each element of this grid. In conventional device simulators (using either the drift-diffusion or the hydrodynamic method) the charge density is usually a generic quantity and the charge assignment problem does not exist. However, in our case, when we have point charges, defining effective charge densities for a Poisson solver implies physical problems:

- If a carrier is assigned to a grid element with a given weight function (W), the original (q) and the assigned charge distributions ($\delta\rho$) are different, thus the potential and the electric field acting on carriers will be different, too. This causes a self-accelerating electric field as one can see in Fig. 2 [1]. Even if we have just a single electron, there will be a given electric field due to the effective charge density assigned to the mesh element where the electron resides. Since the electric field accelerates all charged particles, our single electron would accelerate itself.
- Carriers very close to each other are affected by the same electric field and cannot feel each other's attracting or repelling field. If the speed value or direction of these carriers are only slightly different they can travel together in the structure unless one of them is scattered.
- Another problem arises from the relatively small number of point charges: the assigned charge density can be very rough. This leads to numerical instabilities in the Poisson solver slowing down its convergence.

Line charges vs. point charges. To reduce CPU time consumption, the simulation of physical effects in 3D space can be sometimes simplified by a 2D approach (by taking a unit-width 3-dimensional system, assuming perfect uniformity in the neglected direction).



$$\delta\rho(\mathbf{r}) = \frac{q}{V_c} W(\mathbf{r} - \mathbf{r}_p)$$

$$\mathbf{F}(\mathbf{r}) = \sum_p q W(\mathbf{r} - \mathbf{r}_p) \mathbf{E}(\mathbf{r}_p)$$

$$\mathbf{E}(\mathbf{r}_p) = V_c \sum_{p'} \mathbf{d}(\mathbf{r}_p; \mathbf{r}_{p'}) \rho(\mathbf{r}_{p'})$$

$$\mathbf{d}(\mathbf{r}; \mathbf{r}_{p'}) = -\mathbf{d}(\mathbf{r}_{p'}; \mathbf{r})$$

V_c is the volume of the domain

Figure 2: Charge assignment for the solution of Poisson's equation

This simplification causes that the charges in this model are considered as line charges for which the field has an $1/r$ character and the potential has a logarithmic character, whereas for point charges these are $1/r^2$ and $1/r$, respectively (see the corresponding potentials in Fig. 3).

The effect of this difference can be neglected over large distances, but it is questionable if such a simplification can be applied for a submicron MOSFET where all dimensions are in the order of magnitude of a half micron. Since the force acting on carriers is proportional to the field, the calculated trajectories in the 2-dimensional case are essentially different from the real 3-dimensional ones.

Our approach for potential calculation. To eliminate the previously mentioned problems, the so-called *molecular dynamics method* (in which all charges – including dopant ions – are treated as point charges without charge assignment) seems to be the best suitable technique. However, it is more time consuming and requires more computing power.

A unique feature of the MiCroMOS program is that the $\mathbf{E}(\mathbf{r})$ field and the $\Psi(\mathbf{r})$ potential distributions are calculated *without solving Poisson's equation*. We apply another method which is detailed below.

Both the electric field and potential are divided into two parts, one originating from the charges inside the Monte Carlo simulated region (and from the $Si - SiO_2$ interface), and the other ($\Psi_B(\mathbf{r})$) caused by the external voltages (boundary conditions):

$$\Psi(\mathbf{r}) = (\Psi_n(\mathbf{r}) + \Psi_p(\mathbf{r}) + \Psi_{imp}(\mathbf{r}) + \Psi_{int}(\mathbf{r})) + \Psi_B(\mathbf{r}) \quad (1)$$

- The field and potential arising from charges in the active region and at the $Si - SiO_2$ interface are analytically determined by using the Gaussian law:

$$\Psi_{n,p,imp,int}(\mathbf{r}) = \pm \frac{q}{4\pi\epsilon} \sum_j \frac{1}{|\mathbf{r} - \mathbf{r}'_j|} \quad (2)$$

$$\mathbf{E}_{n,p,imp,int}(\mathbf{r}) = -\text{grad } \Psi_{n,p,imp,int}(\mathbf{r}) \quad (3)$$

The potential caused by the charged particles can be seen in Fig. 4.



350 Software Applications in Electrical Engineering

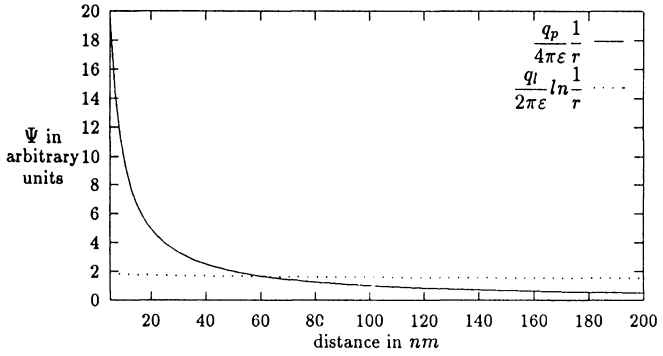


Figure 3: Potential of point and line charges

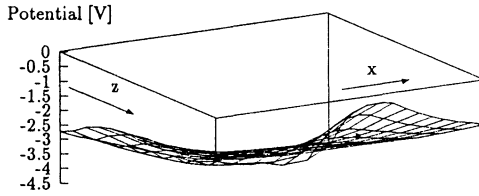


Figure 4: The potential component caused by the charged particles

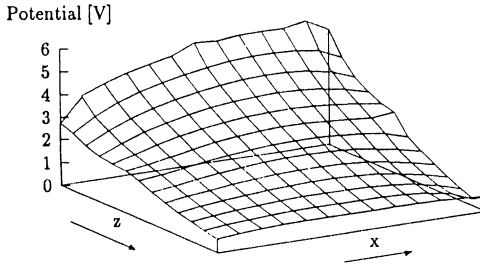


Figure 5: The potential component arising from the solution of the Laplace equation

- The field and potential due to external voltages (ie. the boundary conditions at the Monte Carlo simulated region) are determined by solving the Laplace equation

$$\text{div grad } \Psi_B(\mathbf{r}) = 0. \quad (4)$$

- Satisfying the boundary conditions is assured by the solution of the Laplace equation for modified boundary conditions. The physical boundary condition (basically determined by the external voltages) is given by $\Psi_{ph}(B)$. Thus the modified boundary condition for surfaces with constant potentials at boundary B is obtained by subtracting the potential values given by the electrons, holes, ionized impurities and interface states from $\Psi_B(\mathbf{r})$, ie.

$$\Psi_B(B) = \Psi_{ph}(B) - (\Psi_n(B) + \Psi_p(B) + \Psi_{imp}(B) + \Psi_{int}(B)). \quad (5)$$

For the $Si - SiO_2$ interface the boundary condition is the following

$$\epsilon_{sem} \cdot \mathbf{grad} (\Psi_{charges} + \Psi_{Laplace}) \cdot \vec{n}|_{semi} = \epsilon_{ins} \cdot \mathbf{grad} (\Psi_{charges} + \Psi_{Laplace}) \cdot \vec{n}|_{ins} \quad (6)$$

The potential component arising from the solution of the Laplace equation is shown in Fig. 5

The total potential (the sum of the potential caused by the charged particles and the potential given by the solution of the Laplace equation) can be seen in Fig. 6. These results were obtained for a device structure corresponding to Fig. 1, under the conditions detailed in Table 1.

The advantage of this method is self-explanatory: without solving Poisson's equation directly – which would result in self-accelerating carriers, as shown earlier – the exact field caused by point charges is calculated *analytically* for all carrier positions. Only the Laplace equation must be solved numerically. This enables exact simulation of carrier trajectories and thus the exact evaluation of all Coulomb scattering processes.



352 Software Applications in Electrical Engineering

Parameter		Value:	
L	(Channel length)	0.25E-06	<i>m</i>
D	(Channel depth)	0.30E-06	<i>m</i>
W	(Channel width)	0.25E-06	<i>m</i>
D_drain	(Depth of the drain)	0.12E-06	<i>m</i>
d_ox	(Oxide thickness)	4.50E-09	<i>m</i>
NA	(Substrate doping)	1.00E+23	<i>m</i> ⁻³
ND	(Source/drain doping)	1.00E+24	<i>m</i> ⁻³
Nss	(Surface state density)	-1.00E+15	<i>m</i> ⁻²
Gate		A1	
<i>U_{ds}</i>	(Drain-source voltage)	0.50E+00	<i>V</i>
<i>U_{gs}</i>	(Gate-source voltage)	2.50E+00	<i>V</i>

Table 1: Parameters of the structure used in the potential calculations (see Figures 4–6).

Carrier dynamics

The carrier motion is described by the classical Newtonian law of motion

$$\frac{d^2\mathbf{r}}{dt^2} = \underline{m}_{eff}^{-1} \mathbf{F} \quad (7)$$

where

$$\mathbf{F} = \pm q\mathbf{E} \quad (8)$$

The effect of the magnetic field is neglected.

The second integral of Eq. (7) determines the carrier path. Applying a time increment Δt small enough to assume a constant force during this period, the integration for determining the carrier trajectories can be carried out by a first order numerical quadrature formula:

$$\mathbf{r}(t + \Delta t) = \mathbf{r}(t) + \mathbf{v}(t)\Delta t + \frac{1}{2} \cdot \underline{m}_{eff}^{-1} \mathbf{F}(\mathbf{r}, t) \cdot \Delta t^2, \quad (9)$$

or in a slightly different form

$$\mathbf{r}(t + \Delta t) = \mathbf{r}(t) + \underline{m}_{eff}^{-1} \left[\mathbf{p}(t) + \frac{1}{2} \mathbf{F}(\mathbf{r}, t) \Delta t \right] \Delta t \quad (10)$$

The particle momentum at the time instant $t + \Delta t$ is

$$\mathbf{p}(t + \Delta t) = \mathbf{p}(t) + \mathbf{F}(\mathbf{r}, t) \Delta t \quad (11)$$

For various kinds of carriers different reciprocal effective mass tensors are used. It is assumed that:

1. The reciprocal effective mass tensors are diagonal.
2. The diagonal elements of the reciprocal effective mass tensors are independent of the \mathbf{k} -vector ($\mathbf{p} = \hbar \cdot \mathbf{k}$, \hbar is Planck's constant) and their values correspond to the zero energy surface.

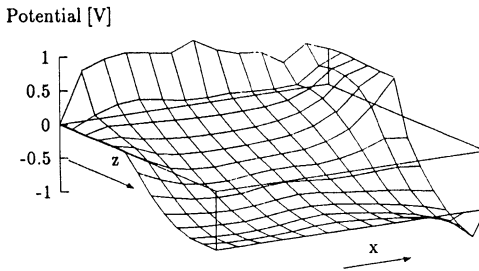


Figure 6: The total potential in the structure. See Table 1. for the structure parameters and the applied voltages.

For electrons, there exist six ellipsoid-shaped constant energy surfaces. For a $\langle 100 \rangle$ oriented crystal, the principal axis of these ellipsoids lies on the positive or negative coordinate axes in the k -space and the centers of constant energy ellipsoids are located at $0.85 |k|_{max}$.

For holes, the diagonal elements are equal, because of the spherical symmetry of the constant energy surfaces. It means, that a scalar effective mass can be considered. Different effective masses are used for the light and heavy holes. The centers of the constant energy surfaces are located at the origin of the k -space, thus the hole velocity vector is directly proportional to the k -vector.

Scattering processes

The advantage of our approach to the potential and field calculation is apparent: since for each charged particle the exact electric field is analytically determined, the charged particle interactions are *inherently* accounted for. This results in the exact simulation of ionized impurity scattering, scattering on charged interface states and carrier-carrier scatterings. Consequently, the real carriers trajectories are automatically followed.

In order to *derive* scattering rates in the post-processing phase of our program, an empirical factor must be used to make a decision whether the change of the direction in the movement of a particle is large enough to consider it as a Coulomb scattering or not.

In the present state of the program the phonon scatterings are modelled quite simply. In the future, more sophisticated models should be applied to take into account real phonon spectra.

For the intervalley scattering of the electrons a thermodynamic approach is applied. For surface scattering, the following phenomena are taken into consideration:

- the Coulomb scatterings caused by charged interface states (as mentioned earlier),



354 Software Applications in Electrical Engineering

- elastic or specular surface scatterings occur if a carrier reaches the $Si - SiO_2$ interface.

The ratio between the elastic and specular surface scatterings are controlled by the so-called Fuchs parameter. This is the only empirical parameter used in our method so far.

The entire simulation algorithm is summarized by the flowchart presented in Fig. 7.

CONSEQUENCES OF OUR SIMULATION METHOD

Since we have point charges, the conventional terms such as *charge density* or *dopant profile* cannot be interpreted in the usual way. This means that a continuum view cannot be applied any more, eg. in a $1 \mu m^3$ volume of Si assuming a doping density of $10^{24} m^{-3}$ there are only 10^6 dopants resulting in 100 particles over a $1 \mu m$ length. However, it is possible to define methods which would match macroscopic parameters used by process engineers (eg. doping profile) to our microscopic view.

Due to our approach the conventional technological input data need to be pre-processed and the macroscopic output parameters (currents, mobilities) should be identified by means of statistical post-processing of our calculated results.

DISCUSSION OF RESULTS

With the method applied in MiCroMOS all the carriers are individually traced both in the real space and the k -space at each simulation time instant. The carrier-carrier and carrier-ionized impurity interactions, together with some other scattering processes are simulated with no approximation. During the development of our method we mainly concentrated on applying the deepest possible *first physical principles* in the active device region.

The simulation is based on the effective mass concept. As long as this concept is valid, the results can be considered as an exact description of the real physical processes.

Statistical evaluation

Special postprocessor programs are used to evaluate the results (to convert our detailed results into "human readable" format for people used to classical device simulators). There are tools to calculate the drain current components and the RMS noise of the drain current; regression analysis of number of carriers, electrons entering to drain, the average time spent in the active region; the cross correlation between the initial and final positions during a single simulation step, and the averaged velocity components; distribution of electrons between different ellipsoids vs. time spent in structure; distribution of the electron temperature vs. time spent in structure; statistics of scattering rates; estimation about mobility components; etc.

Test run results

With the first working version MiCroMOS [3], we performed test runs on DEC's new, 7000-series machines built around the 64-bit Alpha chips. Based on the detailed results obtained from these runs we calculated the net drain current and the electron mobility in the inversion channel. The applied voltages were as follows: $U_{ds} = 0.5 V$ and $U_{gs} = 2.5 V$.

The runs were performed on the test structure shown in Fig. 8. The structure parameters are summarized in Table 2 (see Fig. 8 for the notations).



Software Applications in Electrical Engineering 355

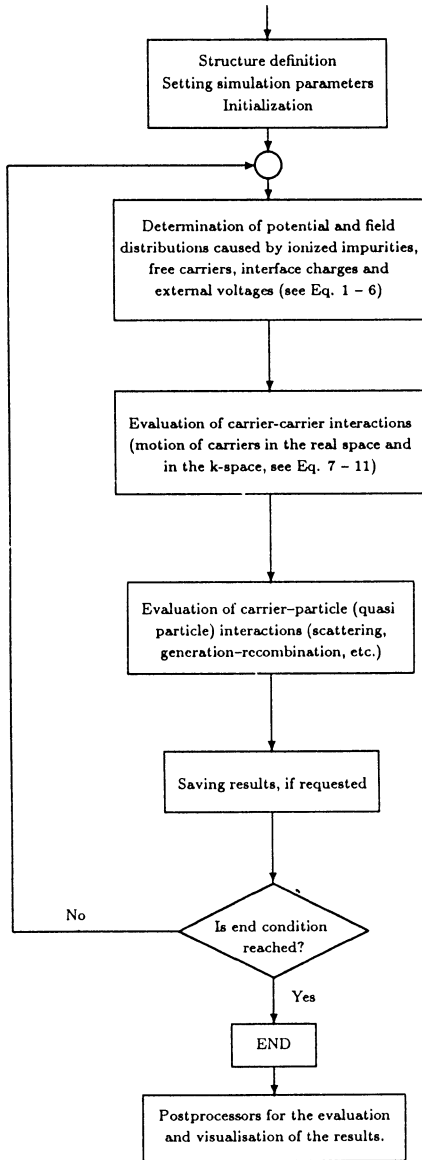


Figure 7: The flow chart of the MiCroMOS program



356 Software Applications in Electrical Engineering

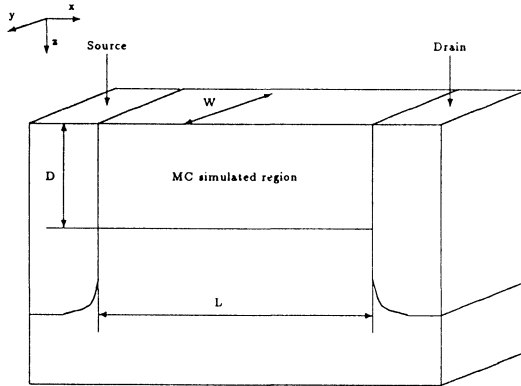


Figure 8: The structure used for testing the first version of the MiCroMOS program.

Parameter	Value:
L (Channel length)	2.33E-07 m
D (Channel depth)	3.00E-07 m
W (Channel width)	5.00E-07 m
d.ox (Oxide thickness)	4.50E-09 m
NA (Substrate doping)	1.00E+23 m ⁻³
ND (Source/drain doping)	1.00E+24 m ⁻³
Nss (Surface state density)	-1.00E+15 m ⁻²
Gate	Al

Table 2: Parameters of the structure used for our test runs.



Software Applications in Electrical Engineering 357

Valley	I_d [μA]	$\delta I_d / \delta t$ [$\mu A / s$]	I_{noise} [μA]
< 1, 0, 0 >	1.8065	0.0047	0.2937
< -1, 0, 0 >	4.1291	-0.0116	0.4091
< 0, 1, 0 >	18.4951	0.0276	0.8725
< 0, -1, 0 >	20.0435	-0.0050	0.8900
< 0, 0, 1 >	6.9679	-0.0136	0.5522
< 0, 0, -1 >	24.3447	0.0113	1.0348
Σ	75.7868	0.0133	1.9454

Table 3: Results concerning the I_d drain current *derived* from the detailed simulation results of the MiCroMOS program.

Scattering type	Scattering rate [ps^{-1}]	Mobility [m^2 / Vs]
Lattice scattering	6.5924	0.0831
Impurity scattering	1.6333	0.3355
Interface state scattering	0.0000	-
Electron - electron scatt.	1.3363	0.4101
Electron - hole scatt.	0.0000	-
Elastic surface scattering	2.0193	0.2714
Specular surface scattering	1.9599	0.2796
Resulting mobility (Mathesian rule)		0.0406
(multiple scatterings accounted once)		0.0487

Table 4: The scattering rates and mobility values *resulting* from the statistical evaluation of the carrier trajectories. An averaging was performed for the entire device structure.

In Table 3 portions of detailed simulation reports concerning the drain current I_d are presented. Note that the different current components represented by electrons belonging to different valleys are distinguished.

In addition to the drain current, mobility values can also be obtained. In Table 4 we summarized *derived* scattering rates and the resulting mobility values.



358 Software Applications in Electrical Engineering

References

- [1] R.W. Hockney and J.W. Eastwood: *Computer Simulation Using Particles* Adam Hilger, Bristol and Philadelphia, 1988
- [2] C. Jacoboni and P. Lugli: *The Monte Carlo Method for Semiconductor Device Simulation* Springer Verlag, Wien New York, 1989
- [3] Tarnay, K. – Masszi, F. – Kocsis, T. – Poppe, A. – Verhás, P.: *Quantum Mechanical Approach for the Examination of the Properties of MOS Inversion Layers in p-type Silicon* Proceedings of the 15th NORDIC SEMICON (Hämeenlinna, Finland), pp. 187-190., June, 1992.